Available online at www.sciencedirect.com
SCIENCE DIRECT®
Journal of Crystal Growth 277 (2005) 143–148
JOURNAL OF CRYSTAL GROWTH
www.elsevier.com/locate/jcrysgro

From Si nanotubes to nanowires: Synthesis, characterization, and self-assembly

T. Qiu[a,b], X.L. Wu[a,*], Y.F. Mei[b], G.J. Wan[b,c], Paul K. Chu[b,**], G.G. Siu[b,**]

[a]*Department of Physics, National Laboratory of Solid State Microstructures, Nanjing University, Han Kou Road 22, Nanjing 210093, People's Republic of China*
[b]*Department of Physics and Materials Science, City University of Hong Kong, Kowloon, Hong Kong, People's Republic of China*
[c]*College of Materials Science and Engineering, Southwest Jiaotong University, Chengdu, People's Republic of China*

Received 19 January 2005; accepted 27 January 2005
Available online 7 March 2005
Communicated by R. Kern

Abstract

Through electroless silver deposition, we have successfully fabricated Si nanowires (SiNWs) in a conventional vessel containing aqueous HF and $AgNO_3$ solution. Their growth mechanisms are analyzed on the basis of a self-assembled localized microscopic electrochemical cell model. A series of scanning electron microscope observations reveal the detailed growth process of the SiNWs. The formation of intermediate Si nanostructures (undetached Si nanotubes) is suggested to be responsible for the growth of triangular shaped SiNWs. The shape and structure of the SiNWs and intermediate undetached Si nanotubes are promising characteristics for applications in interconnection and basic components for future nanoelectronic and optoelectronic devices.

PACS: 61.46.+w; 62.25.+g; 81.07.−b

Keywords: A2. Electrochemical growth; A1. Nanostructures; B2. Semiconducting silicon

1. Introduction

In the past years, a variety of silicon nanostructures have extensively been studied [1,2]. Among them, silicon nanowires (SiNWs) have attracted considerable attention due to their potential applications in interconnection and basic components for future nanoelectronic and especially optoelectronic devices [3–6]. It has been

*Corresponding author. Tel.: +86 25 8359 3702; fax: +86 25 8359 5535.
**Corresponding authors.
E-mail addresses: hkxlwu@nju.edu.cn (X.L. Wu), paul.chu@cityu.edu.hk (P.K. Chu).

0022-0248/$ - see front matter © 2005 Elsevier B.V. All rights reserved.
doi:10.1016/j.jcrysgro.2005.01.095

suggested that the SiNWs thinner than 100 nm in diameter may be used in quantum-wire high-speed field effect transistors and light-emitting devices with extremely low power consumption [7]. Another interesting silicon nanostructure is a silicon nanotube, similar to the existing carbon nanotube. Although a possibility of the existence of silicon nanotubes (SiNTs) has been suggested theoretically, it is very difficult to realize them experimentally due to the favorable formation of sp^3 hybridization of silicon in SiNTs [8]. Some stable silicon tubular structures have been predicted to have electronic structures similar to phosphorous nanotubes, which exhibit semiconducting features independent of the tube diameter and chirality [9]. However, the preparation of SiNTs is still a great challenge so far [10].

Based on the vapor–liquid–solid growth mechanism [11], various techniques have been developed to fabricate SiNWs, mainly including physical deposition, laser ablation, evaporation, and solution methods [12–16]. However, high temperature, hazardous silicon precursors, complex equipment, and other rigorous conditions are often required. Recently, using a nanochannel array of porous alumina template, the SiNTs have been synthesized via molecular beam epitaxy [17] and a conventional catalyst-assisted vapor–liquid–solid process [18]. However, as pointed out in our previous work [19], when using porous alumina templates to fabricate nanostructured materials, it is necessary to carefully distinguish the obtained products from the alumina nanotubes and nanowires. Therefore, it is interesting and of significance to fabricate the SiNWs and SiNTs in the case when the template is not used.

In this paper, we present a relatively rapid method to fabricate the SiNWs. This method arises from electroless metal deposition on a silicon wafer through selective etching. Electroless metal deposition in ionic metal (silver) HF solution is based on micro-electrochemical redox reaction in which both anodic and cathodic processes occur simultaneously at the silicon surface [20]. This is a simple and inexpensive fabrication technique and has been widely used in microelectronics and the metal-coating industry [21–23]. Moreover, we also analyze the growth mechanisms of the obtained materials in detail on the basis of self-assembled localized microscopic electrochemical cell model. A series of scanning electron microscope (SEM) observations further disclose the growth details of the SiNTs. Intermediate nanostructures (undetached SiNTs) are found during the Si wafer etching, which suggests that the formation of undetached SiNTs is an intermediate growth process for forming the triangular shaped SiNWs. This formation mechanism is also in good agreement with the localized microscopic electrochemical cell model.

2. Experimental procedure

The sample fabrication method is described as follows: A p-type, B-doped silicon (1 0 0) (1–5 Ω cm) wafer was first cleaned by acetone to degrease the Si surface, followed by etching in diluted aqueous HF solution for 10 min. Then the cleaned silicon wafer was etched in a 5.0 mol/L HF solution containing 0.02 mol/L silver nitrate at 50 °C for 60 min. The container is a conventional Teflon-lined stainless steel vessel. After the etching process, the silicon wafer was rinsed with deionized water and blown dry in air. The thick silver film wrapping the silicon wafer was detached before microstructural observation. The morphology and chemical composition of the samples were characterized with a FEG JSM 6335 field-emission scanning electron microscope (FESEM) and a PHI 5600 X-ray photoelectron spectrometer (XPS) with a monochromatic AlKα source at 14 kV and 350 W. The photoelectron take-off angle was 45°. All the measurements were performed at room temperature.

3. Results and discussion

Fig. 1(a) shows the cross-sectional SEM image of the etched silicon wafer. We can see that the oriented SiNWs are perpendicular to the surface of the Si wafer and have a uniform distribution. The etched depth (i.e. the lengths of SiNWs) of the Si wafer is approximately 20 μm. The diameters of nanowires are in the range of 30–200 nm. We also

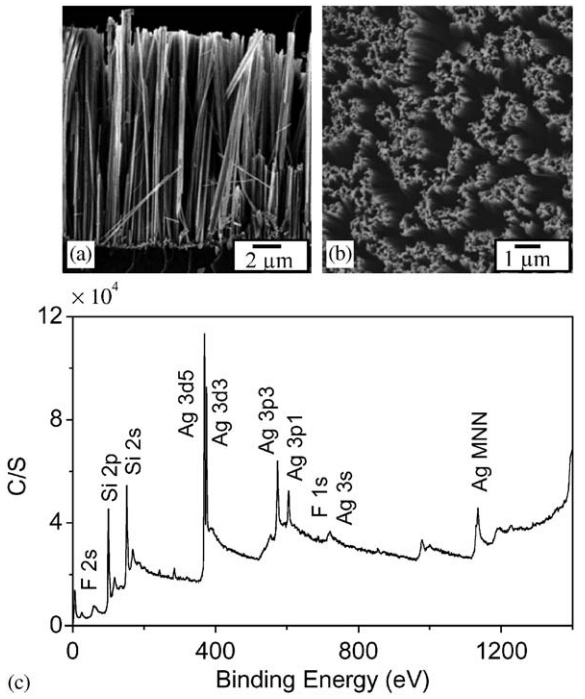

Fig. 1. (a) Cross-sectional SEM image of Si nanowire array. (b) SEM image of large-area silver-capped SiNWs. (c) XPS spectrum acquired from etched silicon wafer at the sputtered depth of ~10 nm.

found that each Si nanowire has a cap-like nanolayer on the free end. Their morphologies can be observed in Fig. 1(b), which shows large-area SiNWs. To determine the elemental composition and chemical states of the nanolayer, we carried out the XPS measurements of the etched silicon wafer. To remove the surface contamination, we used Ar ions to bomb the sample surface for several minutes (remove the surface layer of about 10 nm) and then measured the XPS spectrum. The corresponding result is presented in Fig. 1(c). Obviously, the main element in the nanolayer is Ag except for a slight amount of Si. The XPS result displays the evidence for the existence of silver nanolayers (Ag nanoparticles like caps) on the SiNWs.

Formation of the silver-capped SiNWs can be understood on the basis of self-assembled localized microscopic electrochemical cell model [24] and diffusion-limited aggregation process [25]. Fig. 2

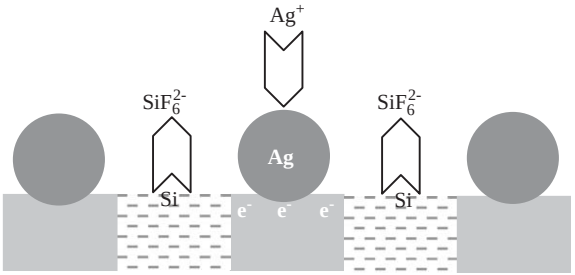

Fig. 2. Schematic diagram of the etching process of silicon wafer in silver nitrate HF solution.

gives a schematic diagram of their formation process in silver nitrate HF solution. At the initial stage, silicon etching and silver deposition occur simultaneously at the Si wafer surface. The deposited silver atoms first form nuclei and then form nanoclusters which are uniformly distributed on the surface of the silicon wafer. These silver nanoclusters and the Si areas surrounding these silver nuclei could, respectively, act as local cathodes and anodes in the electrochemical redox reaction process, which can be formulated as two half-cell reactions (1) and (2):

$$Ag^+ + e^- \rightarrow Ag, \quad (1)$$

$$Si + 6F^- \rightarrow SiF_6^{2-} + 4e^-. \quad (2)$$

That is to say, numerous nanometer-sized free-standing electrolytic cells could be spontaneously assembled on the surface of the silicon wafer in aqueous HF solution. Unlike other metal nanoclusters such as Pt, Cu, Fe, etc., which have a strong tendency to coalesce and form a continuous grain film in the process of electroless metal deposition, silver nanoclusters deposit on the surface of silicon wafer to form tree-like dendrites [26], which involves cluster formation by the adhesion of a particle with random path to a selected seed on contact and allows the particle to diffuse and stick to the formed structure [25]. In situ prepared SiNWs around the silver nanoclusters could be regarded as the template that is something like Xiao's work about ultrasonically assisted template synthesis of palladium and silver dendritic nanostructures [27]. With the progress of silver deposition, silver nanoclusters acting as the

cathodes are successfully preserved, while the surrounding silicon acting as the anodes is etched away. Thus, the presence of these nanoscale electrolytic cells leads to selective etching of the silicon substrate.

To further identify the growth process of the SiNWs, we performed more SEM observations on intermediate Si nanostructures. Fig. 3(a) shows a cross-sectional SEM image of the etched silicon substrate. We can see that the surrounding silicon acting as the anodes has been etched away to form the channel (by the arrows). The diameters of the channels are in the range of 80–300 nm. Compared with ordinary porous silicon, the geometrical shapes of the electroless etched silicon can be produced intentionally if we control the geometrical shapes and positions of local cathodes. The situation is something like the formation of ordering honeycomb structures during anodization of the Al sheet with surface arrangement-ordered nanomasks [19].

In Fig. 3(b), we can also clearly see some nanopores (by the dotted arrow) formed during electroless silver deposition. Inner diameters of the nanopores are in the range of 50–150 nm. Silver nanoclusters as the cathodes can also be found on the top of the nanopore walls (by the solid arrow). In fact, these nanopores and their surrounding silicon constitute the undetached SiNTs. The nanochannels shown in Fig. 3(a) are obviously the central pores of the broken SiNTs which have not been undetached.

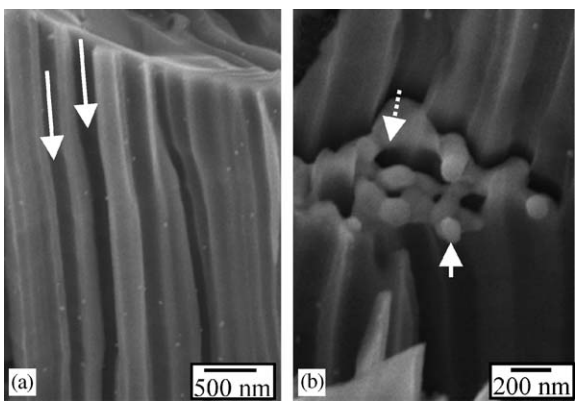

Fig. 3. SEM images of: (a) silicon nanochannels; and (b) undetached SiNTs.

Generally speaking, the areas surrounding the deposited silver nanoclusters which act as anodes are etched like honeycombs. Fig. 4(a) shows the schematic diagram of the growth process of the SiNTs. At the start, the silicon etching and silver deposition occur simultaneously at the silicon surface. Many small flat honeycombs form around one tiny deposited silver nanocluster, that is to say, numerous nanosized honeycomb-like anodes and one silver nanocluster acting as local cathode form an electrochemical cell. These cells could be self-assembled on the surface of the silicon wafer. The synchronous growth of silver dendrites in the process of silver deposition could consume a large quantity of superfluous deposited silver atoms and hold back the coalescence of silver nanoclusters [26]. Thus, most of the silver nanoclusters will keep their sizes. Honeycombs around the silver nanoclusters are etched larger and deeper. Many of them incorporate to form one nanopore. If the silicon wall between two nanopores has not yet been etched completely, that is, the nanopore boundary still consists of a thin silicon wall, as shown in Fig. 4(a), the undetached Si nanotube forms. These undetached SiNTs are something like undetached alumina nanotubes in porous alumina membrane. Alumina nanotubes can be easily detached from membrane by ultrasound vibration [28]. Therefore, we may adopt similar experiments to get individual SiNTs.

Further etching of intermediate undetached SiNTs will lead to the formation of specially shaped SiNWs. Fig. 4(b) shows the schematic diagram of the further etching process of undetached SiNTs. We can see that silicon honeycombs

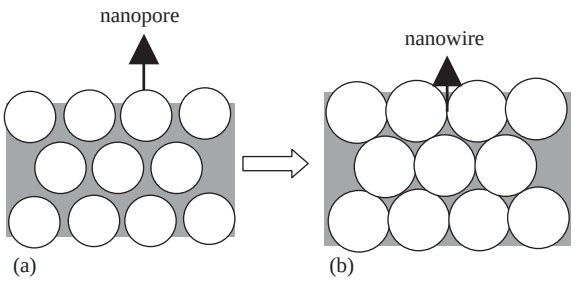

Fig. 4. Schematic diagram of the growth process from SiNTs to SiNWs.

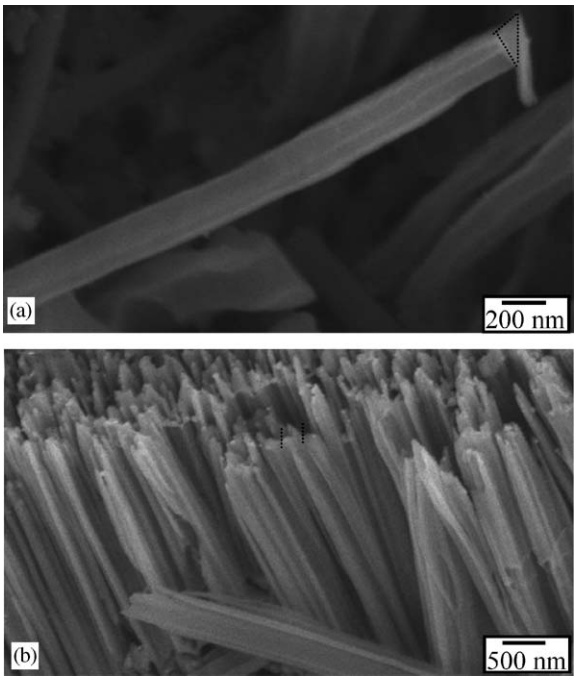

Fig. 5. SEM images of: (a) individual Si nanowire; and (b) large-area SiNWs.

around the silver nanoclusters acting as anodes can be completely etched away, which leads to a connection of many nanopores. As a result, many triangular shaped SiNWs form. Direct experimental evidence in this aspect is shown in Figs. 5(a) and (b). Fig. 5(a) shows a SEM image of individual Si nanowire. One end of the Si nanowire is in triangular shape which is in good agreement with the aforementioned etching mechanism. The SiNWs with residual tube walls can be observed in Fig. 5(b), which results in a large span of Si nanowire diameters in SEM images.

4. Conclusion

In summary, a rapid, inexpensive method of fabricating large-area silver-capped SiNWs has been described on the basis of electroless metal deposition technique without the use of template. Undetached SiNTs were also observed as intermediate products. Self-assembled localized microscopic electrochemical cell model can be used to explain our experimental results well. The shape and structure of Si nanowires and nanotubes are promising characteristics for applications in interconnection and basic components for future nanoelectronic and optoelectronic devices.

Acknowledgments

This work was supported by the Grants (nos. 10225416 and 60476038) from the National Natural Science Foundation of China and by Hong Kong Research Grants Council (RGC) Competitive Earmarked Research Grants (CERG) #CityU 1137/03E and CityU 1120/04E, and CityU University of Hong Kong Strategic Research Grant (SRG) #7001642.

References

[1] J. Hu, M. Ouyang, P. Yang, C.M. Lieber, Nature 399 (1999) 48.
[2] U. Landman, R.N. Barnett, A.G. Scherbakov, P. Avouris, Phys. Rev. Lett. 85 (2000) 1985.
[3] Y. Cui, C.M. Liber, Science 291 (2001) 851.
[4] Y. Cui, Q.Q. Wei, H.K. Park, C.M. Lieber, Science 293 (2001) 1289.
[5] M. Paulose, C.A. Grimes, O.K. Varghese, E.C. Dickey, Appl. Phys. Lett. 81 (2002) 153.
[6] T. Qiu, X.L. Wu, X. Yang, G.S. Huang, Z.Y. Zhang, Appl. Phys. Lett. 84 (2004) 3867.
[7] B. Marsen, K. Sattler, Phys. Rev. B 60 (1999) 11593.
[8] S.B. Fagan, R.J. Barierle, R. Mota, A.J.R. Da Silva, A. Fazzio, Phys. Rev. B 61 (2000) 9994.
[9] G. Seifert, T. Köhler, H.M. Urbassek, E. Hernández, T. Frauenheim, Phys. Rev. B 64 (2001) 193409.
[10] R.Q. Zhang, S.T. Lee, C.K. Law, W.K. Li, B.K. Teo, Chem. Phys. Lett. 364 (2001) 251.
[11] R.S. Wagner, W.C. Ellis, Appl. Phys. Lett. 4 (1964) 889.
[12] T.I. Kamins, R.S. Williams, Y. Chen, Y.L. Chang, Y.A. Chang, Appl. Phys. Lett. 76 (2000) 562.
[13] A.M. Morales, C.M. Lieber, Science 279 (1998) 208.
[14] N. Wang, Y.F. Zhang, Y.H. Tang, C.S. Lee, S.T. Lee, Appl. Phys. Lett. 73 (1998) 3902.
[15] G.C. Xiong, H.T. Zhou, S.O. Feng, Appl. Phys. Lett. 72 (1998) 3458.
[16] J.D. Holmes, K.P. Johnston, R.C. Doty, B.A. Korgel, Science 287 (2000) 1471.
[17] S.Y. Jeong, J.Y. Kim, H.D. Yang, B.N. Yoon, S.H. Choi, H.K. Kang, C.W. Yang, Y.H. Lee, Adv. Mater. 15 (2003) 1172.

[18] J. Sha. J. Niu, X. Ma, J. Xu, X. Zhang, Q. Yang, D. Yang, Adv. Mater. 14 (2002) 1219.
[19] X.F. Shao, X.L. Wu, G.S. Huang, T. Qiu, M. Jiang, J.M. Hong, Appl. Phys. A (2005).
[20] P. Gorostiza, M.A. Kulandainathan, R. Diaz, F. Sanz, P. Allongue, J.R. Morante, J. Electrochem. Soc. 147 (2000) 1026.
[21] R. Sard, Y. Okinaka, H.A. Waggener, J. Electrochem. Soc. 136 (1989) 462.
[22] D.B. Wolfe, J.C. Love, K.E. Paul, M.L. Chabinyc, G.M. Whitesides, Appl. Phys. Lett. 80 (2002) 2222.
[23] A. Hilmi, J.H.T. Luong, Anal. Chem. 72 (2000) 4677.
[24] K.Q. Peng, Y.J. Yan, S.P. Gao, J. Zhu, Adv. Funct. Mater. 13 (2003) 127.
[25] T.A. Witten Jr., L.M. Sander, Phys. Rev. Lett. 47 (1981) 1400.
[26] K.Q. Peng, Y.J. Yan, S.P. Gao, J. Zhu, Adv. Mater. 14 (2002) 1164.
[27] J.P. Xiao, Y. Xie, R. Tang, M. Chen, X.B. Tian, Adv. Mater. 13 (2001) 1887.
[28] T. Qiu, X.L. Wu, G.S. Huang, G.G. Siu, Y.F. Mei, F. Kong, M. Jiang, Thin Solid Films 476 (2005) 210.